



VOL. 10 NO. 5 DECEMBER, 2019 ISSN: 1074-4741

International JOURNAL OF Engineering & Research Technology



EDITOR-IN-CHIEF
Prof. Saeid Eslamian [IRAN]
Department Head of Water Engineering
Isfahan University of Technology, Iran.



KINETICS STUDIES OF QUICKLIME PRODUCTION FROM CALCINED OYSTER

SHELL USING MAMPEL'S RATE LAW

G.A. AYASHIM, J. ADUKWU, H. UTHMAN

Department of Chemical Engineering, School of
Infrastructure, Process Engineering and Technology
P.M.B 65, Main campus, Gidan kwano, Minna, Niger
State, Nigeria.

Abstract

Calcium oxide (CaO) is accepted as an effective adsorbent of carbon dioxide (CO₂), and it is commonly used in biodiesel production. Calcium carbonate (CaCO₃) sources, such as limestones that are obtained through mining and quarrying, usually produce CaO. CaO is produced via thermal decomposition. However, this research has been able to use the vast available waste resources for CaCO₃ and CaO in Nigeria, which is Oyster shells. Kinetic study of the thermal decomposition of the Oyster shell using Mampel power rate law. The model was then used to study the effect of Oyster shell particle size, calcination time and calcination temperature on activation energy of the thermal decomposition of the shell in a calciner. It was found that while the activation energy of thermal decomposition of Oyster shell decreased from 169.164958kJ/mol to 128.1852 kJ/mol as the particle size of Oyster increased from 0.3

mm to 2.0 mm, the activation energy of thermal decomposition of Oyster shell decreased from 66.46616491 to 44.3326 kJ/mol as the calcination time of Oyster increased from 60 min to

KEYWORDS: oyster
shell, kinetics,
mampel, calcination

180 min, and the activation energy of thermal decomposition of Oyster shell decreased from 150.84 kJ/mol to 11.7543332 kJ/mol as the calcination temperature of Oyster increased from 600 °C min to 900 °C. To conclude, a promising source of CaO is the Oyster shell, which provides the largest decomposition rates for small particle size, higher calcination temperature and higher residence time.

Introduction

Morton (1997) stated that oysters belong to the phylum mollusks or mollusks and to the class gastropods, a large group of invertebrate animals. Oysters live among wet vegetation in damp and shady places,

they are more abundant in rainy seasons and most active at night. The oyster's soft body consists of a head, a foot, and a visceral mass or lump, which remains permanently inside a hard protective shell. Most gastropods have a single usually spirally coiled shell, into which the body can withdraw, when the oyster's body is drawn into the shell, it is sealed by a Horney plate called the operculum. Oysters are highly diverse in size, anatomical structure as well as in behavior and habitat (Morton, 1997). Oysters are characterized by a soft body, usually with an exoskeleton in the form of a shell as shown in figure 1. The shells provide protection for the soft-bodied inhabitants against predators (Kaplan, 1998). The shell has a brownish color with a characteristic stripe pattern.

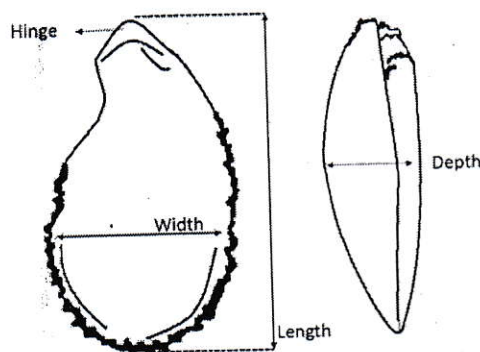
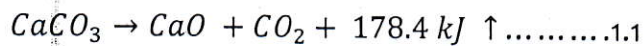


Figure 1; oyster frontal and side views

The main constituent of the shell is calcium carbonates which are either of two crystalline forms calcite and aragonite. The remainder is organic matrixes which constitute a protein known as conchiol in that usually make up to 5% of the shell (Jordaens et al., 2007). The shell is upto 10 cm or more in length, it is very hard. A lot of them also live in fresh water and terrestrial habitats. Oyster shell has several important uses, which results from the hard nature of the shell. The shell protects the oyster from physical damage, predators and dehydration. They are use also in the manufacture of buttons, quicklime, jewels, and art collections (Jatto et al, 2006). The composition of the Oyster shell is similar to that of Oyster shell lends the effects of it as an alternative to Oyster shell for production of quicklime. It is scientifically known that the Oyster shell is mainly composed of compounds of calcium. As previously mentioned, calcium carbonate (CaCO_3), is the major composition of the Oyster Shell, accounting for 98% of the total composition of the Oyster shell. Similarly, calcium carbonate is the primary raw material in the production of quicklime (Marinoni et al. (2012); Yusuf (2015), Bello (2015); Akande

(2015). It is, therefore, indicated that Oyster shell and Oyster Shells have the same primary composition in calcium compounds. On the basis of the common compositional characteristics of Oyster shell and limestone, it was reasoned in this study that the calcinations of the Oyster Shells could produce high quality quicklime.

Quicklime is majorly produced by thermal dissociation of CaCO_3 based material (calcium carbonate, snail shell, Periwinkle and Calcium carbonate) calcination with the release of carbon dioxide:



Craig (2010) presented three essential factors in the kinetics of calcium carbonate calcinations. To ensure complete calcination, these factors are required and these include;

1. Dissociation temperature of the carbonate must be uniform throughout the entire stone.
2. Minimum dissociation temperature must be exceeded throughout the period of the calcinations process.
3. Carbon dioxide gas evolved in the process must be removed.

With this factors in mind, the particle size, time of reaction and the temperature of the reaction are key kinetic parameter for complete and effective conversion of CaCO_3 based material to CaO

Consequently, the calcinations of Oyster Shell, with a focus on determining the settings of calcinations parameters that will simultaneously optimize quicklime yield and quality with minimal variation was investigated (Akande, 2015).

MATERIALS AND METHODS

MATERIALS: Oyster shell, nitrogen, silica gel, platinum crucible, mortar and pestle, lithium bromide

METHODOLOGY

Sample preparation: Oyster shell sample was repeatedly washed to remove dirt and other impurities material, and subsequently dried in oven at temperature of 40°C . The dried oyster shell was crushed in a jaw crusher after which the oyster shell was grinded to very small particle size and sieved into a particle size of 0.30mm, 0.60mm and 2.0mm respectively. It was then placed into the reactor

where the calcination process takes place with respect to the effect of process variables.

Experimental Design:

Thermal decomposition of Oyster shell was assumed to follow a Mampels Power Rate Law Kinetic model. When calcination is performed in the presence of CO₂, the re-carbonation of quicklime also occurred as shown in eqn(1.1).
The equation describes the kinetics of this reversible reaction.

$$\frac{dX_{CaCO_3}}{dt} = k_1 S a_{CaCO_3} - k_{-1} S a_{CaO} P_{CO_2} \quad 3.2$$

where X_{CaCO_3} is the fraction of CaCO₃ remaining in the sample at reaction time t (minutes), S is the area at reaction interface, a_{CaCO_3} and a_{CaO} are the activities of CaCO₃ and CaO; k_1 and k_{-1} are forward and reverse reaction rate constants (min⁻¹); t , P_{CO_2} (kPa) is the partial pressure of CO₂ in the calcination gas. X_{CaCO_3} is defined by equation 3.3 where m_i and m_f are the initial sample mass and final mass(kg) at the termination of reaction, m is the mass (kg) remaining at reaction time t (time) and α is the mass conversion.

$$X_{CaCO_3} = 1 - \frac{m_i - m}{m_i - m_f} = 1 - \frac{m_i - m}{m_i - m} = 1 - \alpha \dots \dots 2.1$$

Determination of kinetic parameters

Kinetic parameters for thermal decomposition of Oyster shell samples can be determined by Mampel Power Rate Law model (MPRLM).

Power Rate Law Model

Therefore, the kinetic analysis of the calcination of Oyster shell was done. Few process variables were studied such as temperature, duration time, particle size and heating rate. In a gas-solid reaction, Arrhenius equation is applied for kinetic analysis. Hence, in the kinetic analysis of calcination reaction, a combination of equations is used as shown in equations (2.2) and (2.3).

$$d(\alpha)/d(t) = kf(\alpha) \quad 2.2$$

$$\ln k = \ln A - \frac{E_a}{R} \left(\frac{1}{T} \right) \quad 2.3$$

Based on Equation (2.3), Arrhenius equation is written in a linear form, where k represents specific rate constant, A is pre-exponential factor, E_a is activation energy of the process (J/mol), R is universal gas constant (8.314 J·K⁻¹·mol⁻¹) and T is absolute temperature in Kelvin. Meanwhile, the unit of pre-exponential factor

is identical to the specific rate constant and will vary depending on which reaction order is being used. Rearranging Equations (2.2) and (2.3), a new Arrhenius equation is formed as shown in Equation. (2.4).

$$\ln[(d\alpha/dt)/f(\alpha)] = \ln A - \frac{E_a}{R} \left(\frac{1}{T}\right) \quad 2.4$$

According to Samtani *et al.*, (2002) value of $f(\alpha)$ is dependent on types of reaction order which can be decided upon the best fit curve. Consequently, different Arrhenius plot of $\ln k$ against $1/T$ can be plotted, depending on which kinetic parameter is to be computed. The research work was conducted using zero-order kinetic model as shown in equation 2.5 and accuracy of the curve was assessed by regression coefficient values (R^2).

$$f(\alpha) = (1 - \alpha)^0 = 1 \quad 2.5$$

Besides, the closer value of the coefficient of determination to unity was deemed to provide the best fit. Based on the curve plotted, activation energy was obtained from the slope and meanwhile, y-intercept values indicate the pre-exponential factor.

The slope and intercept would be calculated using the equations below;

$$\text{Slope} = - \left[\frac{\varepsilon_a}{R} \right] \quad 2.6$$

$$\text{Intercept} = \ln(A) \quad 2.7$$

From equations 2.6 and 2.7 activation energy and pre-exponential factor are calculated;

$$\varepsilon_a = -\text{slope} \times R \quad 2.8$$

$$A = e^{\text{Intercept}} \quad 2.9$$

Effect of Calcination Temperature, calcination time and particle size on on A & E_A

The following template was used for the determination of the effect of calcination temperature, calcination time and particle size on on A & E_A

Where;

$$LOI = \frac{A-B}{C} \% \quad 2.10$$

And

$$\alpha = \frac{LOI}{0.4392} \quad 2.11$$

Table 1; calculations for different Arrhenius plot of $\ln k$ against $1/T$, depending on which kinetic parameter is to be computed.

| Exp. Run | Calcination Temperature | Particle size (mm) | Heating Rate ($^{\circ}C/s$) | Calcination Time (min) | A = Mass of oyster shell Sample (g) | B= Mass of empty crucibles (g) | C = Mass of Crucible + Sample Before Calcination (g) | D = Mass of Crucible + Sample After Calcination (g) | LOI = $\frac{(C-D)}{A}$ | $\sigma = \frac{((LOI)/0.4932)}$ | $\frac{da}{dt}$ | $\frac{(da/dt)}{f(a)}$ | $1/T$ | $\ln(da/dt)/f(a)$ |
|----------|-------------------------|--------------------|--------------------------------|------------------------|-------------------------------------|--------------------------------|--|---|-------------------------|----------------------------------|-----------------|------------------------|-------|-------------------|
| 1 | | | | | | | | | | | | | | |
| 2 | | | | | | | | | | | | | | |
| 3 | | | | | | | | | | | | | | |
| 1 | | | | | | | | | | | | | | |
| 2 | | | | | | | | | | | | | | |
| 3 | | | | | | | | | | | | | | |
| 1 | | | | | | | | | | | | | | |
| 2 | | | | | | | | | | | | | | |
| 3 | | | | | | | | | | | | | | |

RESULTS AND DISCUSSION

Effect of Calcination Process Factors on Kinetic Parameters

Bogwardt (1995) reported that high yield of quicklime from thermal decomposition of $CaCO_3$ based material such as Oyster shell relies primarily on the furnace, calcination state (temperature, time and particle size of the Oyster shell) and the composition of the Oyster shell. Researchers Bogwardt (1995); Harison (1992); Potgieter *et al.* (2003); Baxiotis *et al.* (2011); Akande (2015) indicated that process variables (Temperature of calcination, time of calcination and particle size of the Oyster shell) are responsible for producing quicklime and thermal decomposition of the $CaCO_3$ based material. This research, therefore, tends to examine the kinetic study of thermal decomposition of Oyster shell. The effect of calcination temperature, oyster shell particle size and calcination time on activation energy of thermal decomposition of Oyster are shown below.

Effect of Oyster shell Sizes on Kinetic Parameters

The effect Oyster shell varied particle sizes (0.3 mm to 2.0 mm) on the activation energy of Oyster shell thermal decomposition are shown in Table 3.1. The values shown in Table 3.1 of the activation energies and pre-exponential variables were obtained from the slope and intercept of Figure 3.1 – 3.3. From the result it can be

deduced that the activation energy decreased from 169.16 kJ / mol to 128.19 kJ / mol as the particle size of the Oyster shell increased from 0.3 mm to 2.0 mm. During the calcination reaction, the finest particle (0.3 mm) is reported to agglomerate. The surface area of the material limits the heat and mass transfer that requires a high energy barrier to be overcome while the greater surface Oyster shell with increased heat and mass transfer during calcination makes the energy barrier low to be overcome.

Table 3.1: Effect of Oyster Shell Particle Sizes on Activation Energy from Thermal Decomposition of Oyster Shell

| Particle Size (mm) | E_A (kJ/mol) | A (mg/min) | R^2 |
|--------------------|----------------|-------------|--------|
| 0.3 | 169.164958 | 490041186.7 | 0.9932 |
| 0.6 | 159.903162 | 89254286.01 | 0.9876 |
| 2.0 | 128.185252 | 1056001.327 | 0.9992 |

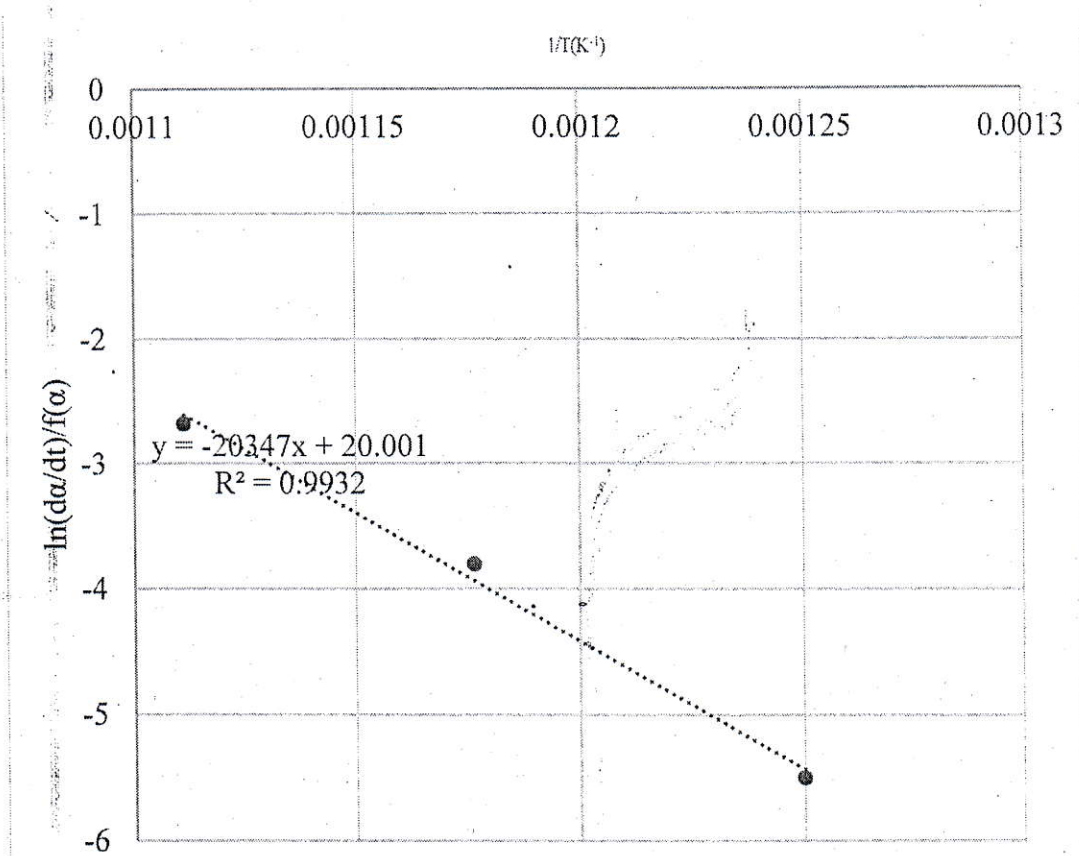


Figure 3.1: The plot of $\ln (d\alpha/dt)/f(\alpha)$ against $1/T$ for obtaining kinetic parameters for a sample of particle sizes of 0.3 mm using zero-order reaction mechanism.

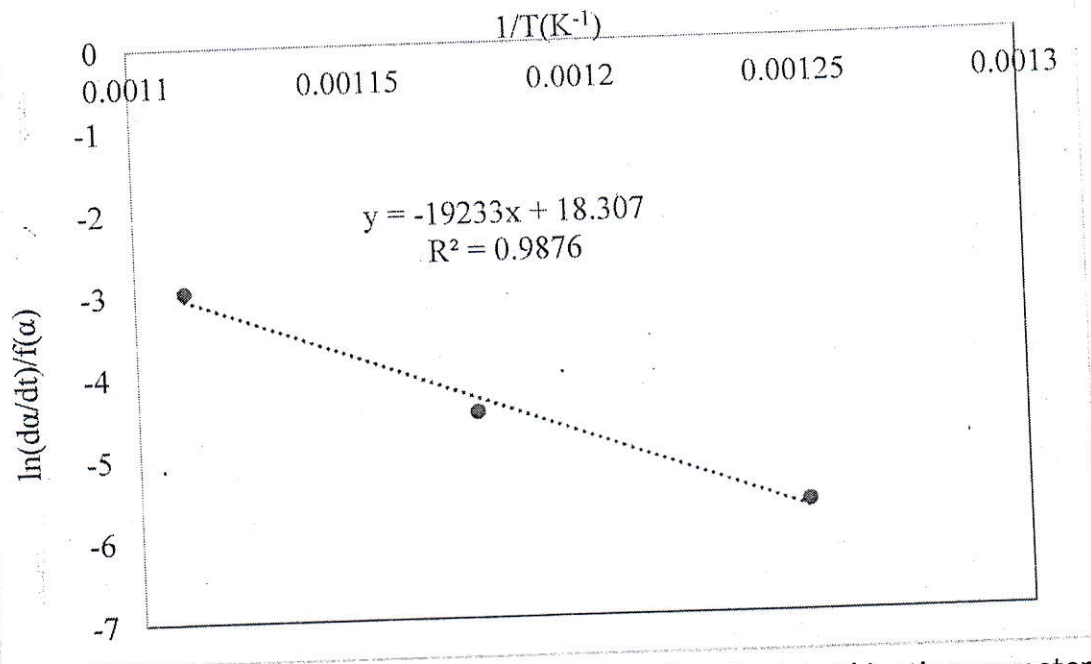


Figure 3.2: The plot of $\ln (d\alpha/dt)/f(\alpha)$ against $1/T$ for obtaining kinetic parameters for a sample of particle sizes of 0.60 mm using a zero-order reaction mechanism.

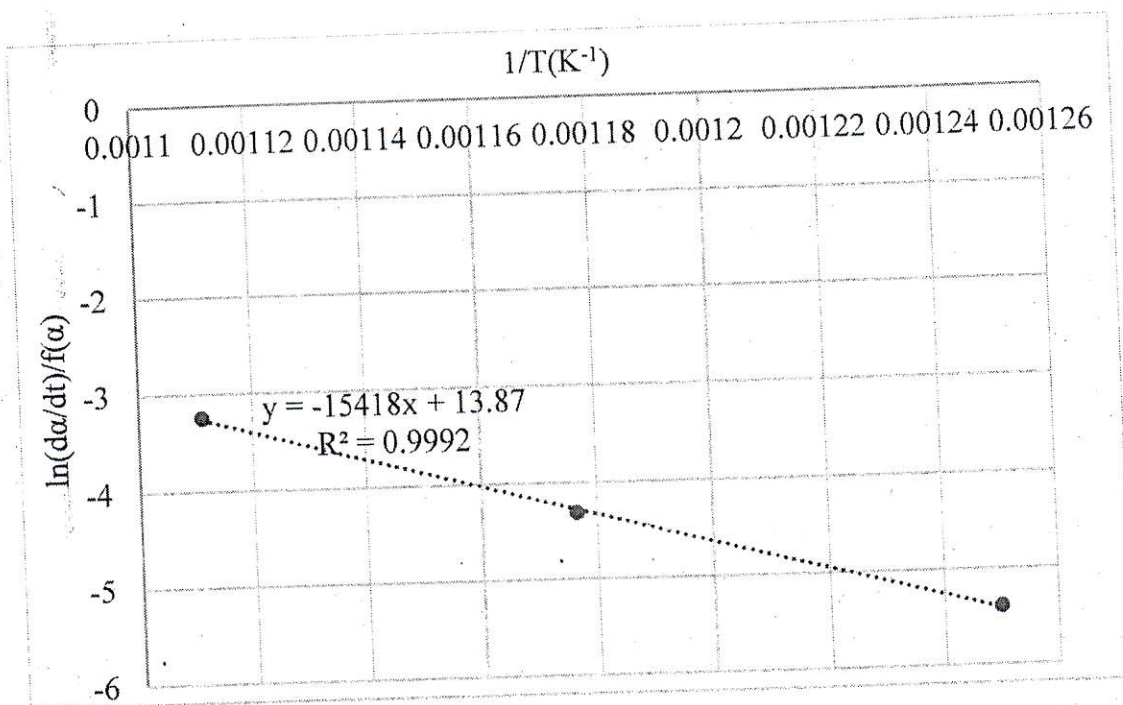


Figure 3.3: The plot of $\ln(da/dt)/f(\alpha)$ against $1/T$ for obtaining kinetic parameters for a sample of particle sizes of 2.0 mm using a zero-order reaction mechanism. Borgwardt (1985) stated that the calcination process would be controlled by kinetic reaction and therefore the reaction rate would be proportional to the surface area of the BET. In addition, the sample's largest surface area will radically enhance the heat distribution with them, thereby increasing the process of better decomposition; therefore, the resistance to the reaction is decreased, resulting in low activation energy. According to the, particle size will have a reaction and mass transfer restriction, as well as suggesting that the calcination rate will also be strongly affected by the pore structure in which particle size has less pore digestion strength that affects mass transfer to the pores. (Ye *et al.*, 1995). Hassibbi (1999) reports that the particle size distinction affects the sample penetration of the heat. Akande (2015) noted that continuous residence time and calcination temperature, heat will not fully penetrate the bigger samples, resulting in only the exterior layer being transformed to CaO and lower samples remaining at CaCO₃. Furthermore, based on the result obtained in Table 3.1 saturation energy value for the particle size of 0.3 m is higher than the particle size of 2 mm. This demonstrates that the Oyster shell sample surface area can be lowered, thus limiting the heat and mass transfer of the process.

Effect of calcination time on kinetic parameters

Table 4.4 shows the kinetic analysis for Oyster shell samples for different calcination time using the first-order reaction. For the kinetic study, Arrhenius curves were plotted at various calcination time to obtain the value of activation energy and pre-exponential factors from the slope and intercept of the linearized Mampel rate law zero-order reaction mechanism as shown in Figure 3.4-3.6. The result shows a decrease in the activation energy from 66.47 kJ / mol to 44.33kJ/mole as the calcination time increased from 60 minutes to 120 min.

It demonstrates that the energy barrier to be removed from Oyster shell's thermal decomposition is lowest at high calcination time (Akande, 2015), where he indicated that calcination time plays a vital role in achieving the efficiency of Oyster shell's heat decomposition.

In the calcination procedure balancing between calcination temperature and calcination time is desirable, Akande (2015) describes the significance of CaCO₃ residence moment during the calcination phase using the methodology of response surface (RSM) and OVAT method analysis. Short residence time is

reported to have a probability that the CaCO_3 in Oyster shell will not be fully converted into CaO and, on the other hand, long residence times will result in shrinking sample volume resulting in the pores being closed and CO_2 released being restricted from diffusing out of the sample core.

Table 3.2: Effect of Calcination Time on Activation Energy for Thermal Decomposition of Oyster shell

| Calcination Time (min) | E_A (kJ/mol) | A (mg/min) | R^2 |
|------------------------|-------------------|---------------|-----------|
| 60 min | 66.46616491 | 121.0031768 | 0.9925047 |
| 120 min | 52.35106583 | 14.20847901 | 0.9675388 |
| 180 min | 44.33263056 | 3.568709336 | 0.9959843 |

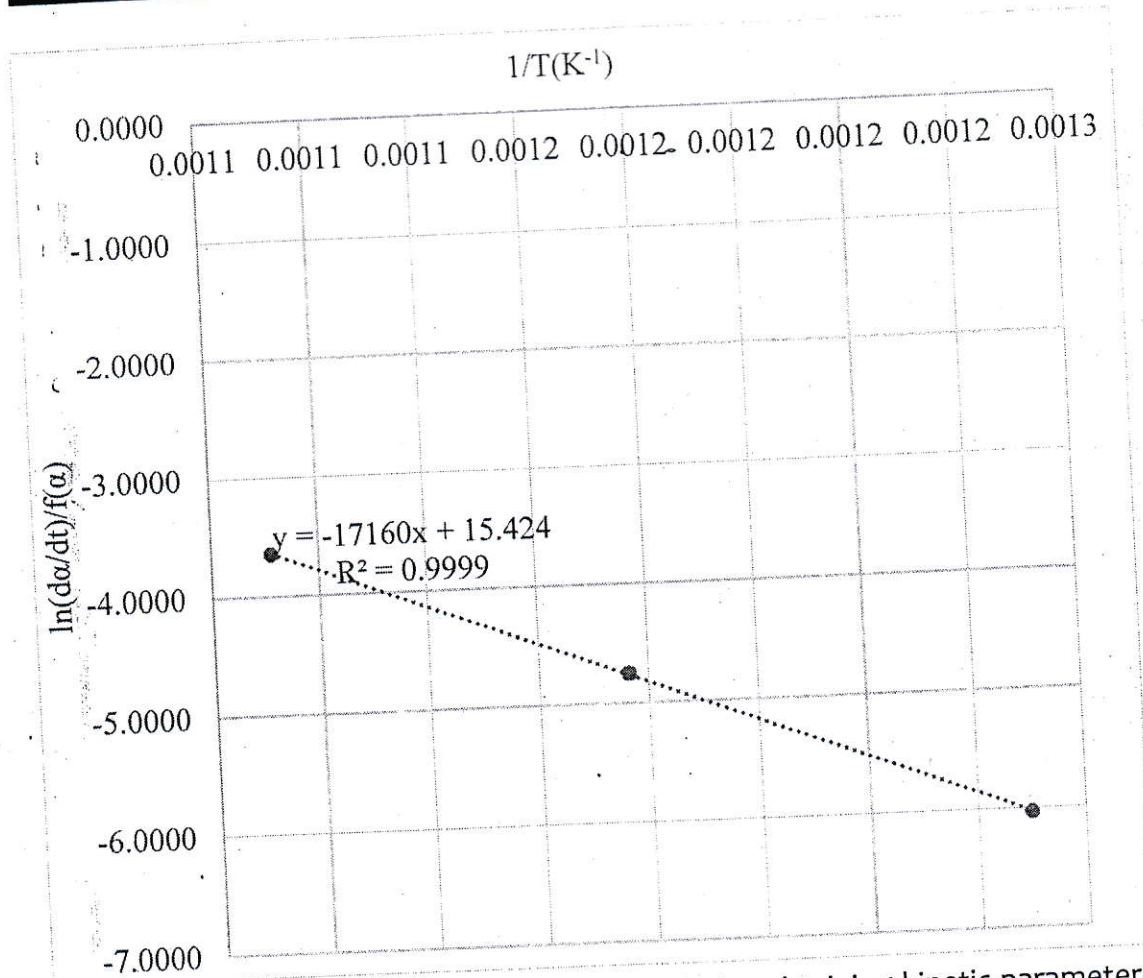


Figure 3.4: The plot of $\ln(da/dt)/f(\alpha)$ against $1/T$ for obtaining kinetic parameters for a sample of calcination time of 60 min.

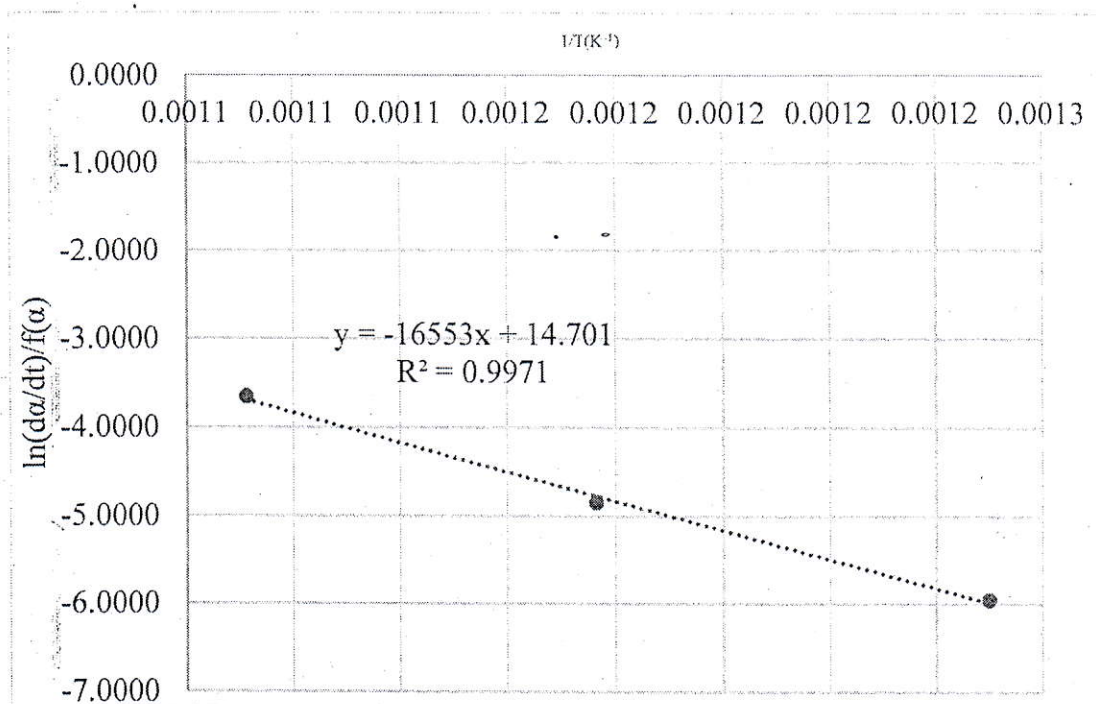


Figure 4.5: The plot of $\ln(da/dt)/f(\alpha)$ against $1/T$ for obtaining kinetic parameters for a sample of calcination time of 120 min.

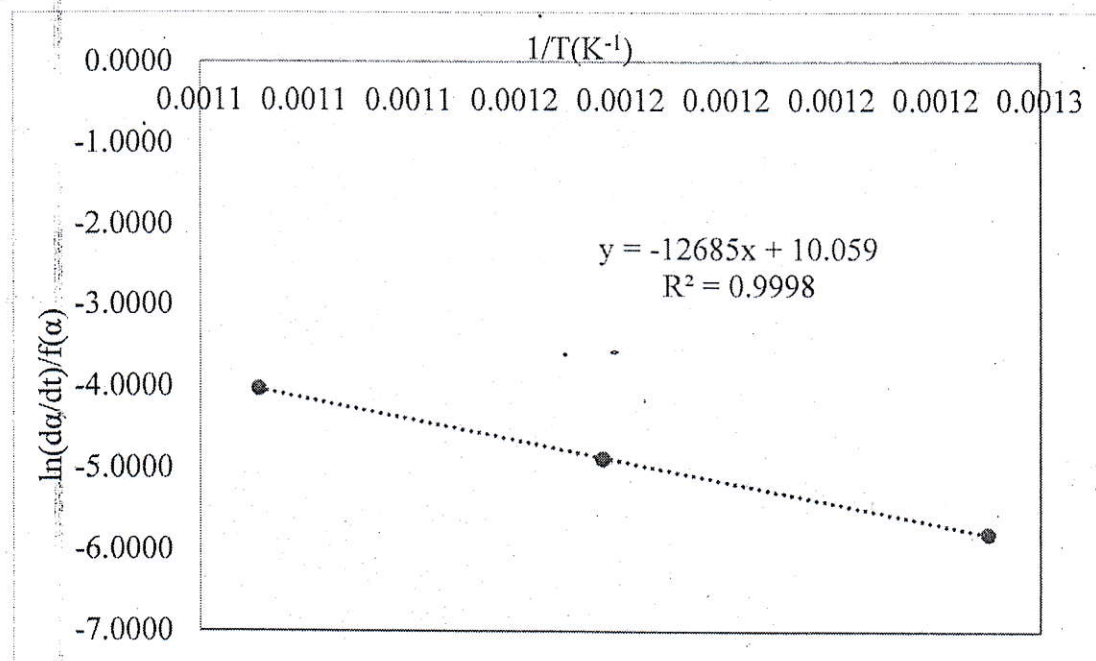


Figure 4.6: The plot of $\ln(da/dt)/f(\alpha)$ against $1/T$ for obtaining kinetic parameters for a sample of calcination time of 180 min.

Effect of calcination temperature on kinetic parameters

The plot of Figure 3.7 to Figure 3.9 shows the kinetic analysis for Oyster shell samples at different calcination temperatures using the zero-order reaction mechanism for the kinetic study, Arrhenius curves were plotted at 3 various calcination temperatures to determine the activation energy values and the pre-exponential factor from the slope and y-intercept of the linearized Mampel rate law.

Table 3.3 shows the kinetic study of Oyster shell samples using the zero-order reaction mechanism at different calcination temperatures. As shown in Figure 3.7 to Figure 3.9, Arrhenius curves were plotted at three distinct calcination temperatures for the kinetic parameters to determine the value of activation energy and pre-exponential factor from the slope and y-intercept of linearized Mampel rate law zero-order reaction process.

Table 3.3: Effect of Calcination Temperature on Activation Energy for Thermal Decomposition of Oyster shell

| Calcination Temperature (°C) | E _A (kJ/mol) | A (mg/min) | R ² |
|------------------------------|-------------------------|-------------|----------------|
| 600 - 700 | 150.840902 | 17470075.43 | 0.9952 |
| 700 - 800 | 51.9151102 | 6.019474722 | 0.9884 |
| 800 - 900 | 11.7543332 | 148.8144161 | 0.9687 |

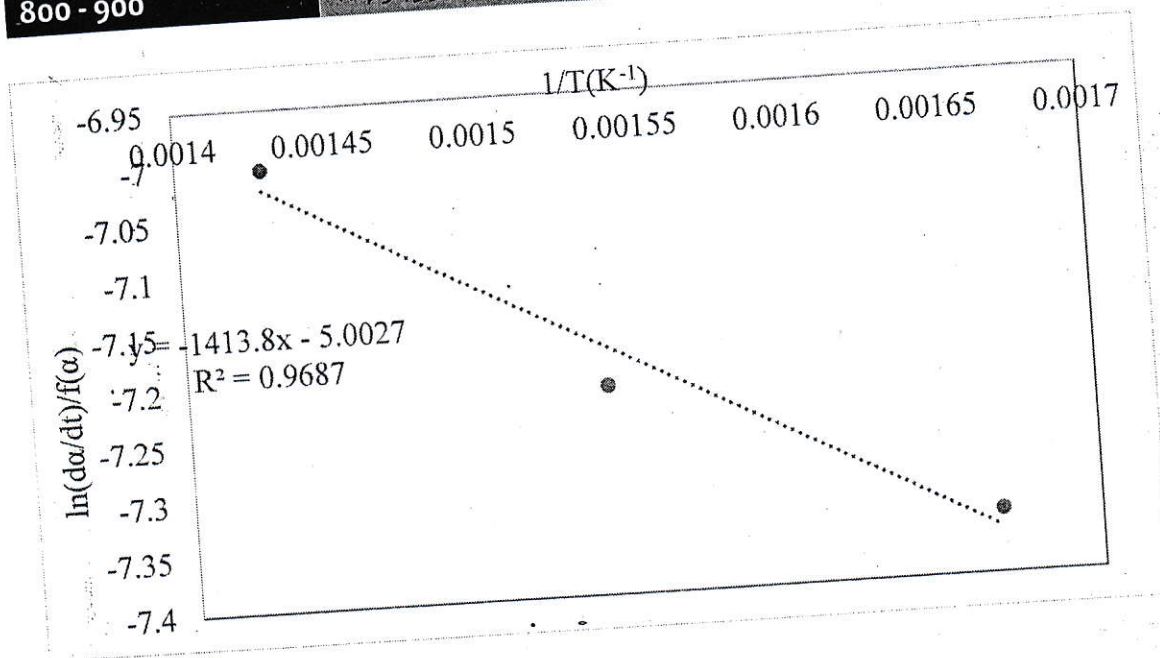


Figure 3.7: The plot of $\ln(d\alpha/dt)/f(\alpha)$ against $1/T$ for obtaining kinetic parameters for a sample of calcination temperature of 700 °C.

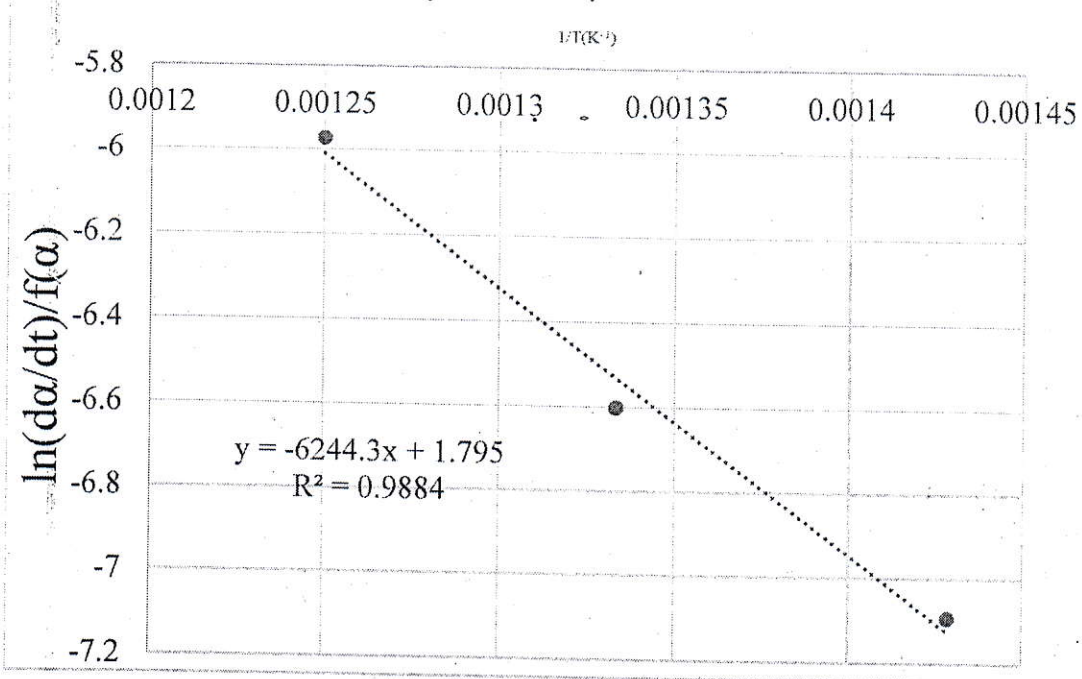


Figure 3.8: The plot of $\ln(d\alpha/dt)/f(\alpha)$ against $1/T$ for obtaining kinetic parameters for a sample of calcination time of 800 °C.

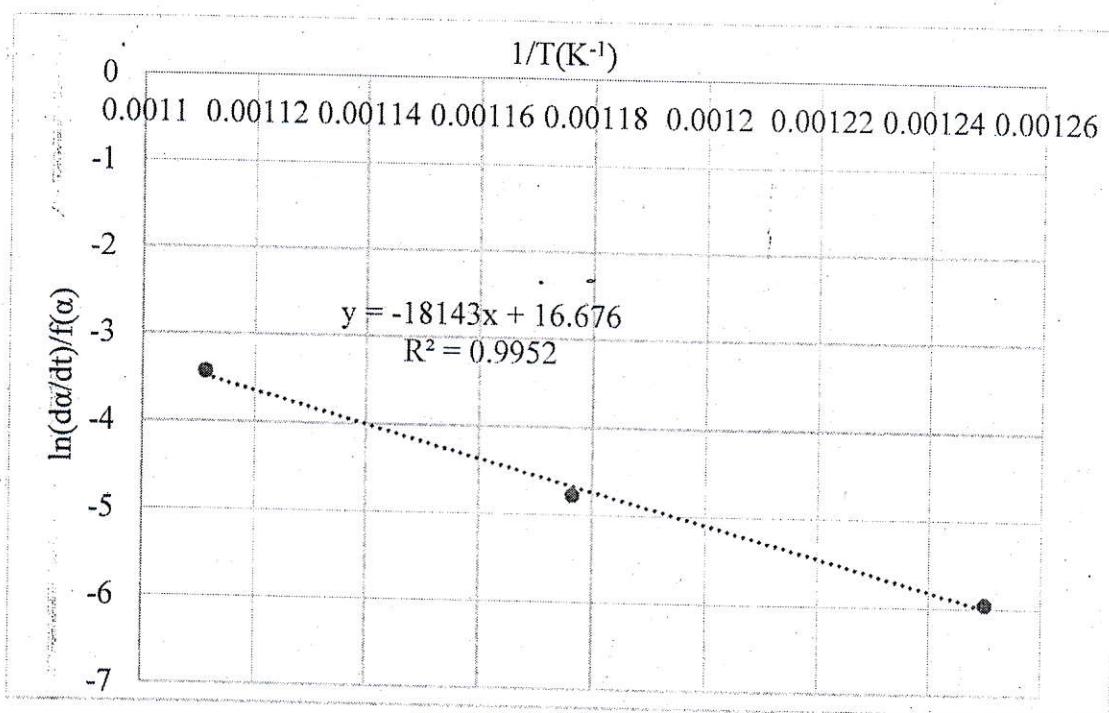


Figure 3.9: The plot of $\ln(da/dt)/f(\alpha)$ against $1/T$ for obtaining kinetic parameters for a sample of calcination time of 900 °C.

The result indicates that the activation energy dropped from 150.84 kJ / mol to 11.75 kJ / mol as the calcination temperature increased from 600 °C to 900 °C. Yusuph et al. (2013) deduced that reduced energy activation values acquired at greater calcination temperature were assigned during calcination to the kinetic energy of the material samples based on calcium carbonate. Yusuph et al. (2013) indicated that the samples have more energy to increase their kinetic energy and the calcination process at greater temperatures. Similar results were also discovered by Abdulqadir (2016) and Kim and Kwon (1998) in which the calcination reaction proceeds slowly at temperatures below 850 °C compared to temperatures above 850 °C. Other works by Li et al. (2003), Telfat et al. (2000), Sakandijan et al. (2007) and Van de Runstarat et al. (1997) also show the trend of increasing activation energy with respect to temperature.

CONCLUSIONS

The study found out that ;

- The activation energy of thermal decomposition of Oyster shell decreased from 169.164958kJ/mol to 128.1852 kJ/mol as the particle size of Oyster increased from 0.3 mm to 2.0 mm.
- The activation energy of thermal decomposition of Oyster shell decreased from 66.46616491 to 44.3326 kJ/mol as the calcination time of Oyster increased from 60 min to 180 min.
- The activation energy of thermal decomposition of Oyster shell decreased from 150.84 kJ/mol to 11.7543332 kJ/mol as the calcination temperature of Oyster increased from 600 °C min to 900 °C.

All the findings were supported by literature and past work done on other CaCO_3 containing materials such as limestone and other sea shells. Further studies can be done to determine the effect of other kinetic parameters such as presence of impurities on the calcination of oyster shell.

REFERENCES

- Akande, H. F. (2015). Multiple Response Optimization of Quicklime Production from limestone using Design of Experiment. Minna: PhD Thesis Federal University of Technology.

- Borgwardt, R. H. and Harvey, D. R. (1985). Properties of Carbonate Rocks Related to SO₂ Reactivity. *Environ Science Technology*, 6, 351.
- Bouineau, V., Pijolat, Y. and Soustelle, M. (1998). Characterization of the Chemical Reactivity of a CaCO₃ powder for Decomposition. *Journal of European Ceramic Society*, 18, 1319-1324.
- Boynton, R. S. (1980). *Chemistry and Technology of Lime and Limestone*. New York: Wiley.
- Britton, H. T., Gregg, S. J. and Winsor, G. W. (1952). The Calcination of Dolomite. Part I — The Kinetics of The Thermal Decomposition of Calcite And of Magnesite. *Transactions of the Faraday Society*, 63-69.
- Chen, C., Zhao, C., Liang, C. and Pang, K. (2007). Calcination and Sintering Characteristics of Limestone under O₂/CO₂ Combustion Atmosphere. *Fuel Processing Technology*, 171-178.
- Craig, R. A. (2010). *Investigating the use of concentrated Energy of Thermally Decomposed Limestone*. Adelaide: PhD Thesis The University of Adelaide.
- Gutschick, K. A. (1995). *Kirk Othmer Encyclopedia of Chemical Technology. ; Volume 19 (Second ed., Vol. 19)*. London: Wiley-Interscience.
- Halikia, I., Zoumpoulakis, L., Christodoulou, E. and Prattis, D. (2001). Kinetic Study of the Thermal Decomposition of Calcium Carbonate by Isothermal Method of Analysis. *The European Journal of Mineral Processing and Environmental Protection*, 1(2), 89-102.
- Hassibi, M. (2009). An Overview of Lime Slaking and Factors That Affects the Process. *Chemco Systems*, 1-19.
- Hu, N. and Scaroni, A. W. (1996). Calcination of pulverized Limestone Particles under Furnace Injection Conditions. *Fuels*, 75 (2), 177-186.
- Ingraham, T. R. and Marier, P. (1963). Kinetics Study on the Thermal Decomposition of Calcium Carbonate. *Journal Chemical Engineering*, 170-173.
- L'vov, B. V. (1997), Mechanism of Thermal Decomposition of Alkaline Earth. *Thermochimica Acta*, 1-16.
- Mallen, A. L. (1956). *Calcination of Penrice Limestone*. Adelaide: PhD Thesis The University of Adelaide.
- Marinoni, N., Allevi, S., Marchi, M. and Dapiaagi, M. (2012). A Kinetic Study of Thermal Decomposition of Limestone Using In Situ High Temperature X-Ray Powder Diffraction. *Journal of American Ceramic Society*, 95(8), 2491-2498.

- Moropoulou, A., Asterias, B. and Aleni, A. (2001). The Effect of Limestone Characteristics and Calcination Temperature to the Reactivity of the Quicklime. *Cement and Concrete Research*, 633-639.
- Muazu, K., Abdullahi, M. and Akuso, A. S. (2011). Kinetic Study of Calcination of Jakura Limestone Using Power Rate Law Model. *Journal of Basic And Applied Science*, 19(1), 116-120.
- Murthy, M. S., Harish, B. R., Rajanandam, K. S. and Kumar, K. Y. (1994). Investigation on the Kinetics of thermal Decomposition of Calcium Carbonate. *Chemical Engineering Science*, 49, 2198-2204.
- Oates, J. H. (1998). *Lime and Limestone: Chemistry and Technology, Production and Uses*. Weinheim: Wiley-VCH.
- Pingsun, J. R., Grace, C. J. and Edward, J. A. (2008). Determination of Intrinsic Rate Constant of the CaO/CO₂ Reaction. *Chemical Engineering Science*, 63, 47-56.
- Potgieter, J. H., Potgieter, S. S. and De Waal, D. (2003). An Empirical Study of factors Influencing Lime slaking: Part II .Influencing of material and water composition. *Water SA*, 29(2), 157-160.
- Rao, T. R., Gunn, D. J. and Bowen, J. H. (1989). Kinetics of Calcium Carbonate Decomposition. *Chemical Eng. Res*, 67, 38-47.
- Rashidi, N. A., Mohammed, M. and Yusup, S. (2012). The Kinetic Model of Calcination and Carbonation of Andara Granosa. *International Journal of Renewable Energy*, 2(3), 497-503.
- Samtani, M., Dollimore, D. and Alexander, K. S. (2002). Comparison of Dolomite Decomposition Kinetics with Related Carbonates and the Effect of Procedural Variable on Its Kinetic Parameter. *Thermochimic Acta*, 6, 392-392.
- Satterfield, C. N. and Feaks, F. (1959). Kinetics of Thermal Decomposition of Calcium Carbonate. *American Institute of Chemical Engineering Journal*, 5, 115-122.
- Shin, H. G., Kim, Y. N. and Lee, H. S. (2009). Effect of Reactivity of quicklime on the properties of hydrated lime sorbent for SO₂ Removal. *Journal of materials Science Technology*, 25, 329-332.
- Soltan, A. M., Awad, S. A. and EL-Ansary, G. M. (2010). Applicability of Egyptian Limestone for Calcination. *Applied Earth Science. Trans. Inst Metall. B*, 119(4), 236-242.
- Wang, Y., Lin, S. and Suzuki, Y. (2007). Study of limestone Calcination with CO₂ Capture: Decomposition Behavior in a CO₂ Atmosphere. *Energy and Fuels*, 21, 3317-3321.